MRI based scoring of the diseased lung
in the preterm infant with BPD

(*UNSEAL BPD* (**UN**iforme **S**coring of the dis**EA**sed **L**ung in **BPD**))

Kai Förster[1,2], Hannah Marchi[3,4], Sophia Stöcklein[5], Olaf Dietrich[5], Harald Ehrhardt[6], Mark O. Wielpütz[7,8], Andreas W. Flemmer[1], Benjamin Schubert[3,9], Marcus A. Mall[8,10,11], Birgit Ertl-Wagner[12], Anne Hilgendorff[1,2, 13]

[1]Division of Neonatology, Dr. von Hauner Children`s Hospital, University Hospital, LMU Munich, Munich, Germany

[2]Institute for Lung Biology and Disease and Comprehensive Pneumology Center (CPC), Helmholtz Zentrum München, Munich, Germany, Member of the German Center for Lung Research (DZL)

[3]Institute of Computational Biology, Helmholtz Zentrum München, Munich, Germany

[4]Chair of Data Science, Faculty of Business Administration and Economics, Bielefeld University, Germany

[5]Department of Radiology, University Hospital, LMU Munich, Munich, Germany

[6]Department of General Pediatrics & Neonatology, Justus-Liebig-University, Giessen, Germany, Member of the German Center for Lung Research (DZL)

[7]Department of Diagnostic and Interventional Radiology, University of Heidelberg, Heidelberg, Germany

[8]Translational Lung Research Center Heidelberg (TLRC), German Center for Lung Research (DZL), Heidelberg, Germany

[9]Department of Mathematics, Technische Universität München, Garching bei München, Germany

[10]Department of Pediatric Respiratory Medicine, Immunology and Critical Care Medicine, Charité-Universitätsmedizin Berlin, Berlin, Germany

[11]German Center for Lung Research (DZL), associated partner site, Berlin, Germany

[12]Department of Medical Imaging, The Hospital for Sick Children, The University of Toronto, Toronto, ON, Canada

[13]Center for Comprehensive Developmental Care (CDeC[LMU]), Social Pediatric Center (iSPZ), Dr. von Hauner Children`s Hospital, University Hospital, LMU Munich, Munich, Germany

Corresponding author:

Anne Hilgendorff, MD
Comprehensive Pneumology Center
Max-Lebsche-Platz 31
81377 München, Germany
Telephone: +49 89 3187 4675; Fax: +49 89 2734 222
E-mail: a.hilgendorff@med.uni-muenchen.de

Abstract

Objective: Neonatal chronic lung disease lacks standardised assessment of lung structural changes.

Method and Results: We addressed this clinical need by the development of a novel scoring system (*UNSEAL BPD* (**UN**iforme **S**coring of the dis**EA**sed **L**ung in **BPD**)) using T2-weighted single-shot fast-spin-echo sequences from 3T MRI in very premature infants with and without bronchopulmonary dysplasia (BPD). Quantification of interstitial and airway remodeling, emphysematous changes and ventilation inhomogeneity was achieved by consensus scoring on a 5-point Likert scale. We successfully identified moderate and severe disease by logistic regression (AUC 0.89) complemented by classification tree analysis revealing gestational age-specific structural changes. We demonstrated substantial inter-reader reproducibility (weighted Cohen's kappa 0.69) and disease specificity (AUC=0.91).

Conclusion: Our novel MRI score enables the standardised assessment of disease characteristic structural changes in the preterm lung exhibiting significant potential as a quantifiable endpoint in early intervention clinical trials and long-term disease monitoring.

Key point: Our new lung MRI score makes semi-quantitative assessment of structural disease characteristics in preterm infants with BPD available for clinical routine, thereby improving current disease grading.

2

Introduction

Chronic lung disease in the preterm infant, i.e., bronchopulmonary dysplasia (BPD), requires clinically applicable diagnostic tools for the standardized assessment of outcome-relevant variables able to predict long-term outcome and with the potential to serve as a much-needed endpoint in clinical trials. To this end, however, clinical practice still solely relies on clinical read-outs of end-stage pulmonary function (1) with limited predictive value while lacking the standardized assessment of structural abnormalities. Whereas conventional chest radiography (CXR) shows low sensitivity and diagnostic value in paediatric and adult lung disease patients (2, 3), the routine application of computed tomography (CT) with high spatial resolution and diagnostic accuracy is limited by radiation exposure (4, 5).

To overcome current diagnostic shortcomings, we developed a novel diagnostic tool for the standardized assessment of disease characteristic structural changes in the BPD lung by taking advantage of the growing opportunities in magnetic resonance imaging (MRI). MRI has not only become the method of choice for diagnosing central nervous system abnormalities in this patient population, but also advanced as a promising strategy to detect structural and functional changes in the diseased lung (6).

In our study *UNSEAL BPD* (**UN**iforme **S**coring of the dis**EA**sed **L**ung in **BPD**), we quantified the disease characteristic and gestational age-related expression of 'emphysema', 'interstitial enhancement', 'airway accentuation', and 'ventilation inhomogeneity' in spontaneously breathing preterm infants with and without BPD near term age. We thereby aimed at informing the clinical BPD diagnosis by more objective disease severity assessment and identification of individual structural changes with potential implications for subsequent monitoring strategies.

3

Patterns and Methods

Cohort of preterm infants with BPD and age-matched controls. Preterm infants ≤ 32 weeks gestational age (GA) with and without BPD were prospectively included in the study after written informed parental consent (n=77 Perinatal Center of the Ludwig-Maximilian University, Campus Grosshadern (EC #195-07); n=17 Perinatal Center of UKGM Giessen (EC#135/12)). BPD was diagnosed based on the definition of the NICHD workshop (7) that identified preterm infants born <32 weeks GA according to their need for supplemental oxygen ($>FiO_2$ 0.21) for at least 28 days, followed by the final assessment at 36 weeks postmenstrual age (PMA) or discharge, whichever came first (disease grading: mild BPD - requirement of supplemental oxygen for 28 days, no need for oxygen supplementation at 36 weeks PMA, moderate BPD - oxygen supplementation $<FiO_2$ 0.30 at 36 weeks PMA, severe BPD - oxygen supplementation $>FiO_2$ 0.30 at 36 weeks PMA and/or positive pressure ventilation/continuous positive pressure) with each treatment referring to continuous application and oxygen supplementation >12 hours equalling one day of treatment (7). Oxygen saturation was assessed by standardized pulse oximetry; no infant was discharged before 36 weeks' gestation.

The clinical course from birth to discharge was comprehensively monitored in all study infants with clinical diagnoses defined as published previously (8) . None of the children received treatment with diuretics or steroids and none of the infants presented with a hemodynamically relevant persistent ductus arteriosus (PDA) at time of MRI. BPD incidences and co-morbidities are indicated in **Table 1**.

119 No significant differences between the cohorts (Perinatal Center of the Ludwig-
120 Maximilian University, Campus Grosshadern and Perinatal Center of UKGM
121 Giessen) were observed regarding GA and birth weight, whereas the duration of
122 mechanical ventilation and oxygen supplementation showed significant differences
123 (student's t-test; $p < 0.05$; **Table 1**). Median age at MRI was 36.1 (range 32.2-51.4)
124 weeks GA (Munich) and 37.1 (range 34.2-43.1) weeks GA (Giessen). Taken both
125 sites together, the median age at MRI was 36.1 (range 32.2-51.4) weeks GA. Thirty-
126 nine percent of the infants were 36 weeks GA +/- 1 weeks at MRI, while the age at
127 MRI in eighty-seven percent were within +/- 1 standard deviation from the median
128 (median: 36.1; SD: 3.9). The images obtained in infants scanned at the age of > 40.0
129 weeks GA showed characteristic imaging features according to the disease grade of
130 the infant when compared to the cases imaged near 36 weeks GA.

131 When comparing BPD grades (no vs. mild BPD, no vs. moderate and severe BPD,
132 mild BPD vs. moderate and severe BPD), GA, birth weight, duration of mechanical
133 ventilation, duration of oxygen supplementation, duration of NICU stay) significantly
134 differed between the groups after testing for outliers and normal distribution
135 (student's t-test; $p < 0.05$) as expected (**Table 1**).

136 **Cohort of infants with cystic fibrosis.** Disease specificity was assessed in a cohort
137 of infants with cystic fibrosis (CF) (n=21, Children's University Hospital Heidelberg
138 (EC #S-370/2011)) (9). The diagnosis of CF was confirmed by increased sweat Cl–
139 concentrations (≥60 mmol/L), Cystic Fibrosis Transmembrane Conductance
140 Regulator (CFTR) mutation analysis, and/or by assessment of CFTR function in
141 rectal biopsies in pancreatic-sufficient patients with borderline sweat test results
142 (sweat Cl–between 30 and 60 mmol/L). Disease severity in CF patients was stratified
143 by pancreatic function (n=16 with exocrine pancreatic insufficiency, median-related
144 age at MRI 195 days (10, 11)).

5

Pulmonary Magnetic Resonance Imaging. Pulmonary MRI was performed at the time of BPD diagnosis, i.e., 36 weeks GA during spontaneous quiet breathing without oxygen supplementation and without invasive or non-invasive respiratory support in supine position swaddled in a vacuum mattress after feeding using neonatal noise attenuators (Minimuffs®, natus® newborn care, Seattle, USA) for hearing protection. Study infants did not exhibit clinical or laboratory signs of infection.

Imaging protocol. 3-Tesla whole-body MRI (Magnetom Skyra, Siemens Healthineers, Erlangen, Germany) was performed with a size-adapted number of coil elements from the 32-channel spine array coil, an 18-channel flexible body array coil and a 20-channel head-and-neck array coil. The protocol included pulse sequences for the qualitative and quantitative assessment of morphology, volume, and structural changes of the lung. In detail, the following pulse sequences were used for the scoring study: T2-weighted single-shot fast-spin-echo (Half-Fourier-Acquired Single-shot Turbo spin Echo, HASTE) sequences in coronal and axial (voxel size 1.3x1.3x4.0 mm³) as well as in sagittal orientations (voxel size 1.2x1.2x4.0 mm³). Echo time (TE) was 57 ms. T2 and the echo time, TE, determine the available signal in the lung parenchyma (12). Acquisitions were electrocardiogram (ECG)-triggered with a minimum repetition time (TR) of two RR intervals; two signal averages were acquired. Parallel imaging with an acceleration factor of 2 was used. In coronal and axial orientation, 20 slices with a field of view (FOV) of 340x255 mm² and a resolution of 256x192 pixels were acquired. In sagittal orientation, 25 slices with a field of view (FOV) of 300x197 mm² and a resolution of 256x168 pixels were acquired. The scan durations of the T2-weighted HASTE sequences varied depending on the cardiac frequency. Typical scan durations were between 30 s and 70 s for each of the three (coronar, axial, sagittal) acquisitions. The average total examination time for lung imaging was ten minutes.

6

171　**Image analysis.** T2-weighted single-shot fast-spin-echo sequences were quantified

172　by a consensus panel (two neonatologists, ≥15 years of professional experience;

173　senior radiologist, >20 years of professional experience) resulting in consensus

174　statements. The reader-based image assessment was performed blinded to the

175　clinical information as achieved by separating image acquisition, pseudonymization

176　and analysis using dedicated medical-imaging monitors certified for radiological

177　reading and diagnostic purposes.

178　Inter-reader variability was assessed in a *second reader study* performed by two

179　independent radiologists, i.e., a third-year radiological resident and a radiology fellow.

180　**Pre-scoring** of all images implemented the following criteria in order to decide about

181　image in- or exclusion:

182　i) Assessment of **technical image quality** including motion artifacts (*i.e.*, a deviation

183　that exceeds the diameter of the structure (*e.g.* vertebrae) by 1.5 times resulted in

184　exclusion of an image for analysis), imaging artifacts (caused by MR-hardware and

185　room shielding, MR imaging software, tissue heterogeneity and foreign bodies,

186　Fourier transform and Nyquist sampling theorem), and a low signal to noise ratio.

187　ii) Presence of **complications** *i.e.,* infiltrates (accumulation of substances such as

188　tissue, material, debris, secretions in the lungs presenting as high signal intensity on

189　T2-weighted images), pneumothorax (any presence of air in the pleural cavity

190　presenting as low signal intensity on T2-weighted images) or pleural effusion (any

191　fluid in the pleural cavity presenting as high signal intensity on T2-weighted images).

192　iii) Assessment of **inflation levels** (1 (normal), 2 (overdistended), 3 (underinflated))

193　describing extremes of the ventilation situation during imaging to establish

194　standardized conditions for the subsequent analysis.

7

195   The presence of insufficient technical image quality and/or one of the indicated

196   complications and/or the described indication of 'overdistension' or 'underinflation'

197   resulted in the exclusion of the MRI scan from analysis.

198   To ensure an appropriate reporting, especially in neonatal imaging the following

199   should be achieved: symmetrical visualization of the thorax, the clavicles and the

200   ribs; visualization of the spine and the paraspinal structures; visual discrimination of

201   the cervical and thoracic trachea, their bifurcation and the central bronchi;

202   visualization of the costo-pleural border from the apex of the lung to the

203   diaphragmatic-rib angle; visual discrimination of the hilar, the heart, and diaphragm;

204   visualization of vascular drawing in the lung core; visual discrimination of vessels

205   possibly down to the lung periphery; avoidance of superimposition of the upper fields

206   by the scapulae; visualization of the thymus.

207   **Morphological MRI score.** Standardized image analysis was performed through

208   scoring of lung morphology based on previous CT- and MRI-score findings (4, 5, 13,

209   14) addressing BPD characteristic structural changes with 'emphysema' and

210   'interstitial enhancement' representing rarefaction and remodeling of the gas

211   exchange area, 'airway accentuation' indicating airway pathology and caudo-cranial

212   or anterior-to-posterior gradients of signal intensities reflecting 'ventilation

213   inhomogeneity'. Presence of 'emphysema' was stated in case of reduced signal

214   intensity, rarefied lung vasculature, hyperexpansion, mosaic pattern of lung

215   attenuation, presence of bullae or blebs; 'interstitial enhancement' was based on

216   distinctive representation of interstitial structures and thickening of broncho-vascular

217   bundles; 'airway accentuation' was reflected by increased signal intensity in the

218   respiratory ducts and scored based

8

219   on airway wall thickness in relation to airway diameter; differences in signal

220   intensities assessed over all lung quadrants in caudo-cranial and anterior-posterior

221   direction were summarised by the variable 'ventilation inhomogeneity' (**Table 2**).

222   Scoring used a *semi-quantitative five-point Likert scale* (15) with a score of '1'

223   representing normal findings, *i.e.,* the absence of any abnormality and a score of '5'

224   indicating maximum pathology. To achieve a high level of standardization, lungs were

225   virtually segmented into four quadrants (upper left, upper right, lower left, and lower

226   right quadrants) based on the dimensions of the lung scan. Scoring was performed

227   for the right and left lung (upper and lower quadrant) in coronal, axial and sagittal

228   axes separately for each variable to allow for the detection of regional differences

229   (**Table 2**).

230   **Statistical analysis.** Statistical analysis was performed using mean values of region-

231   specific readings using R, version 4.0.4. Differences for BPD grades were analysed

232   with Pairwise Wilcoxon test with Bonferroni correction for multiple testing. After

233   removal of outliers, logistic regression analysis was performed comparing i) diseased

234   vs. non-diseased infants and ii) moderate and severe BPD vs. mild and no BPD as a

235   valid approach previously used by other groups (16); dichotomized BPD grades

236   served as binary outcome and the critical clinical confounders (GA and gender (17))

237   and the scoring variables as explanatory variables. Cases with BPD were compared

238   to age matched controls, *i.e.,* preterm infants with initial respiratory distress but no

239   later BPD development. The model performance was inspected by leave-one-out

240   (LOO) cross-validation; final models were used for prediction in the web application.

241   For rule extraction and better interpretability of the underlying structure and

242   interactions of the score values, additionally classification trees (CAR-Trees) were

243   used to identify optimal split points for predictive variables (18). A prediction rule was

244   deducted to detect disease grades using the score obtained for the indicated

9

245   variables. For CART model validation, we used a nested LOO cross-validation with

246   grid hyperparameter tuning to obtain the best performing model for the binary value.

247   The second reader study was assessed using weighted Cohen's kappa. Thirty-six

248   patients from the Munich cohort were included in the second reader study (female

249   n=21, male n=15; median gestational age (GA) was 27.4 weeks (range 24.1-30.6

250   weeks); median birth weight was 920 grams (range 415-1770 grams); no BPD n=20,

251   mild BPD n=9, moderate BPD n=3, severe BPD n=4; median age at MRI scan was

252   35.4 (range 32.2-47.6) weeks GA).

253   **Table 3** shows the results of the logistic regression models (19). Within the logistic

254   regression analysis, the threshold for the negative predictive value (NPV) and the

255   positive predictive value (PPV) were chosen by Youden index (20) when comparing

256   no or mild with moderate or severe cases.

257

Results

Preterm infants (n=94) were prospectively included in the study (n=77 (Perinatal Center, Ludwig-Maximilian University (LMU)), n=17 (Perinatal Center, UKGM Giessen)). Pre-scoring according to standardized quality criteria resulted in the exclusion of n=4 images with insufficient technical quality and n=3 with the presence of complications (pulmonary infiltrates, pneumothorax, pleural effusion, underinflation), resulting in n=87 infants for statistical analysis (n=70 LMU, n=17 UKGM). After removal of statistical outliers (n=3), n=84 infants (n=67 LMU, n=17 Giessen) with and without BPD were available for final analysis (**Table 1; supplemental information Fig. 1, https://figshare.com/s/521ef585ba1d24d2507a**).

In our score, infants with severe BPD demonstrated a significant increase in the incidence of 'emphysema' (p=0.0003), 'interstitial enhancement' (p=0.0002), 'ventilation inhomogeneity' (p=0.042) and 'airway accentuation' (p=0.0039) mirroring disease severity when compared to preterm infants without BPD (**Fig. 1A**).

When combining the scoring variables with the clinical covariates GA and gender to separate moderate and severe BPD from no or mild disease, logistic regression analysis revealed good discriminatory power (AUC 0.89 [0.83; 0.96]) with a NPV of 0.67 and a PPV of 0.93 (threshold chosen by Youden index), thereby explaining significantly more variance than a model only considering clinical variables (GA and gender) (Likelihood ratio test, $\chi^2(4) = 11.50, p = 0.022$). Regression coefficients of the logistic models are included in **Table 3**.

CAR tree (CART) analysis was used to improve interpretability of the results by identifying potential score value interactions. This approach demonstrated disease grade and GA-related characteristic expression patterns of the scoring variables as infants <26.0 weeks GA at birth with moderate or severe BPD were characterised by

11

284   an increased score for ‚emphysema' (split value ≥ 1.88) paralleled by a change in

285   'airway accentuation', in contrast to infants >26.0 weeks GA at birth who exhibited

286   pronounced signs of ‚interstitial enhancement' when diagnosed with moderate or

287   severe BPD (≥ 3.13) **(Fig. 1B)**. Increased 'ventilation inhomogeneity' (split value

288   >1.88) in the presence of lower values for 'interstitial enhancement' (split value <

289   3.13) was shown to separate cases with moderate or severe from no or mild BPD in

290   more mature infants (28th-29th week of GA) (CART AUC 0.69 [0.58; 0.80]; **Fig. 1B**).

291   CART models using clinical (GA and gender) (AUC 0.55 [0.38; 0.73]) or score

292   variables (AUC 0.65 [0.52; 0.79]) alone did not achieve the same performance level.

293   When comparing only the most severe cases to cases without BPD, an AUC of 0.89

294   [0.77; 1] (NPV=0.93; PPV=0.78) was reached, however not significantly

295   outperforming a model only considering clinical variables (Likelihood ratio test,

296   $\chi^2(4) = 6.04,\ = 0.196$). Again, 'interstitial enhancement' was found to separate

297   infants with and without BPD in the infants above 26.5 weeks GA at birth with good

298   discriminatory power (CART split value ≥3.63; AUC 0.87 [0.70; 1.0]; **Fig. 2A**), thereby

299   exceeding the performance of clinical variables only (AUC 0.75 [0.53; 0.97]).

300   A second reader study revealed substantial inter-reader reproducibility (weighted

301   Cohen's kappa of 0.69), referring to a good outcome applying two different levels of

302   proficiency.

303   Disease specificity of the scoring variables (**Fig. 2B**) was shown by comparative

304   analysis using MRI in infants with CF (n=21). CF cases were discriminated from BPD

305   by a decrease in the score values for 'emphysema' and an increase for 'ventilation

306   inhomogeneity' (CART AUC 0.91 [0.82; 0.99], split values <1.13 and ≥1.75) (**Fig.**

307   **2C**)).

308   We translated the standardised assessment of structural findings into a web-based

309   application (https://unsealbpd.helmholtz-muenchen.de/), where the radiologist by

12

310   means of logistic regression analysis is enabled to judge individual scoring results

311   according to their most prevalent association with the disease grade specific

312   expression pattern.

313

314

Discussion

To meet the clinical need for the standardized assessment of structural changes in the BPD lung while avoiding radiation exposure, we developed a routinely applicable MRI-based score in a prospective clinical study. With good sensitivity, specificity, and reproducibility, the score identified disease characteristic and GA-specific structural changes in the BPD lung (21). The findings with fibrosis/interstitial shadows, cystic elements, and hyperinflation in the BPD lung reflect the results obtained by previous imaging studies that used radiation-dependent technology, *i.e.,* CXR and CT (2, 4, 5, 13, 14). Differentiated analysis furthermore revealed distinct structural signatures characterising BPD in different GA groups. Whereas the most immature infants presented with an increased score in 'emphysema' reflecting the rarefaction of the gas exchange area (22) together with a parallel development of 'airway accentuation' scores, the analysis demonstrated 'interstitial enhancement' in infants beyond 26.0 weeks GA at birth, indicating the predominance of fibroproliferative remodeling in these lungs (23). These findings not only provide important pathophysiologic insight but may be of relevance for monitoring strategies and long-term outcome.

Regression analysis and CART models that included the scoring variables exceeded the performance for BPD detection of the models using clinical variables only, underscoring the need to include structural information into the diagnostic process, that currently solely relies on clinical indicators of end-stage pulmonary function (1). The inclusion of GA and gender as covariates into the models though adequately reflected their known impact on BPD incidence (17).

When discussing the score beyond the background of diagnostic alternatives and previous strategies to characterize BPD, different approaches have to be considered including conventional CXR, CT, MRI, and lung ultrasound.

14

340   The current clinical practice to use CXR in the first weeks after birth and during the

341   later course of BPD - mainly based on the lack of diagnostic alternatives - is limited

342   (3, 24) by low sensitivity, high inter-observer variation and reduced predictive value

343   (2, 4, 5, 13, 14, 25). CT, however, benefits from high spatial resolution and

344   subsequent diagnostic accuracy but lacks implementation into clinical routine due to

345   significant radiation exposure (4, 5).

346   The diagnostic value of lung MRI for paediatric and adult patients was demonstrated

347   by studies correlating MRI-based structural information to disease severity (26, 27)

348   and to findings obtained by high resolution CT (26, 28). In infants, MRI-based scores

349   were first developed for cystic fibrosis patients (9, 13), demonstrating applicability of

350   the technique in this age group. In preterm infants, Walkup et al. presented

351   quantifiable differences in signal intensities between preterm infants with (n=6) and

352   without (n=6) BPD as well as full-term controls (n=6) by the use of lung MRI obtained

353   in a small-footprint, 1.5-T scanner (29). Characterisation of lung structural changes in

354   this study was limited by the small cohort size spanning a broad GA range while

355   facing the heterogeneous pathophysiology (22). In addition, the majority of the infants

356   received oxygen supplementation or ventilatory support during image acquisition,

357   impacting MRI results by acting as a paramagnetic agent (12) or by affecting lung

358   aeration. The observation of an increased incidence in emphysema in the BPD lung,

359   however, is in line with our findings. Higano et al. later investigated a cohort of n=42

360   neonates with BPD using ultrashort and gradient echo MRI (16). Here, the high rate

361   of sedation and use of positive-pressure ventilation during MRI limited comparability

362   and thus interpretability of the results. Both MRI studies used a modification of the

363   CT-based Ochiai score (4) that addresses hyperexpansion, emphysema, and

364   fibrous/interstitial abnormalities, thereby potentially neglecting airway pathology and

365   ventilation inhomogeneity.

15

366   In comparison, our study benefited from a larger cohort size, the use of age-matched

367   infants without neonatal chronic lung disease as controls and the standardization of

368   age at MRI to the time of BPD diagnosis (mean GA 36.1 weeks). Comparability and

369   interpretability of the results were improved by avoiding the use of oxygen as well as

370   ventilatory support and by the comprehensive design of the scoring procedure

371   including pre-assessment for image quality, consortial agreement-based scoring, and

372   confirmation of inter-reader reproducibility (4, 16, 29). To best acknowledge the

373   heterogeneous histopathology of BPD (22), we aligned the selection of scoring

374   variables according to previously published radiological markers (13, 16, 21, 30) and

375   applied a more differentiated quantification scale in a total of four lung quadrants. We

376   furthermore took advantage of technical advances to increase image quality while

377   decreasing scanning time. The advances included optimization of signal-to-noise

378   ratio in the high field strength of 3 Tesla (factor 2 when compared to 1.5 Tesla)

379   resulting in improved imaging in small field of views and small voxel dimensions and

380   the use of T2-weighted fast-spin-echo images in three planes leading to greater

381   robustness towards compromises of gradient-echo acquisitions in the lung

382   parenchyma at 3 Tesla. In addition, optimized standard pulse sequences (single-shot

383   fast spin echo) that are available at all installed clinical 3-Tesla scanners (in contrast

384   to newer ultra-short echo-time (UTE) (16) or zero echo time (ZTE) techniques) allow

385   for short examination protocols in a feed-and-sleep technique and thus broad

386   applicability in different centers. Double gating (ECG and respiration) could have

387   improved image quality further, but would have extended imaging time three- to four-

388   fold at the same time. Motion artefacts observed are within a typical range for this

389   patient collective (31) and considered tolerable when pre-scoring excludes significant

390   outliers according to the criteria applied.

391

16

392

393 As motion artifacts are an inherent problem in MRI due to long examination times and

394 sensitivity to motion, these obstacles have driven the development of increasingly

395 faster sequences. There is a general trend toward higher magnetic field strengths as

396 well as long acquisition times to improve spatial resolution. At the same time, these

397 techniques increase the sensitivity to motion artifacts (32). In addition, the

398 dimensions of neonatal structures make them particularly susceptible to motion

399 artifacts as spatial resolution close to or greater than the imaged objects results in

400 contours that often appear inaccurate. Furthermore, even physiological noise sources

401 such as respiration as well as flow and pulse, which are coupled to cardiac cycles,

402 affect image quality (32). In our study, we reduced the impact of artifacts by i)

403 selecting fast imaging sequences and receiver coils, ii) optimally positioning of the

404 patient in the vacuum mattress, iii) tracking infant movements during the imaging

405 process to allow for prospective correction to separate signal from noise and iv)

406 including the impact of motion artifacts in the pre-scoring process.

407 The score`s promising disease specificity, identified by the comparison to a cohort of

408 infants with CF, should be further addressed in studies targeting *e.g.,* infants with

409 congenital diaphragmatic hernia (CDH).

410 In addition to lung MRI, lung ultrasound (LUS) represents a latest diagnostic

411 alternative with predictive value for BPD (n=42 preterm infants GA < 32 weeks GA,

412 16 cases were

413 excluded) as presented by Oulego-Erroz et al. in 2020 (33). The LUS score is based

414 on the semiquantitative assessment of aeration in eight lung zones at the 7th day of

415 life followed by its re-assessment in the fourth week of life. The study is limited,

416 however, by the lack of assessment of other, BPD-characteristic structural

417 abnormalities such as interstitial remodelling and airway pathology, affection of lung

17

418 aeration by altered positions of the infant during LUS and the small number of infants

419 available for final analysis.

420 In summary, our study *UNSEAL BPD* (**UN**iforme **S**coring of the dis**EA**sed **L**ung in

421 **BPD**) enabled the development of an MRI score that adds critical structural

422 information to the current diagnostic concept in neonatal chronic lung disease. The

423 results can inform monitoring strategies in prematurely born infants up into adulthood

424 and may hold the potential to screen for the early appearance of clinically relevant

425 disease phenotypes with impact on lung health later in life (34-36). The identification

426 of differing degrees of fibroproliferation, tissue rarefaction or airway remodelling as

427 well as the identification of GA-dependent structural signatures may cater to the

428 identification of individual risk scores and personalised treatment strategies. In line

429 with this, the score-based identification of infants with severe structural changes that

430 do not correspond to higher BPD grades according to the clinical definition seemingly

431 limits predictive power of the score in some group comparisons. The observation

432 could indicate, however, the score`s potential to reveal structural changes not

433 reflected by clinical BPD grade but of likely relevance for future lung growth and

434 function.

435 Future studies are needed to assess the score's potential to serve as a standardized

436 instrument in clinical studies or to track effects of established perinatal treatments

437 (37, 38). Complementing the structural score by the MRI-based assessment of *e.g,*

438 cardiovascular complications (39-41) might broaden possibilities for clinical use,

439 supported by the web-based application that likely increases the number of use

440 cases.

441 **Acknowledgement**

442 The graphical abstract was created with BioRender.com.

443

18

444

445

Funding

450

Disclosures

Dr. Dietrich reports non-financial support from Siemens Healthineers, outside the submitted work.

Dr. Wielpütz reports grants from Vertex, grants from Boehringer Ingelheim, outside the submitted work.

Dr. Mall reports grants from German Federal Ministry of Education and Research , grants from Einstein Foundation Berlin, during the conduct of the study; personal fees from Bayer, personal fees from Boehringer Ingelheim, personal fees from Polyphor, personal fees from Arrowhead Pharmaceuticals, personal fees from ProQR Therapeutics, personal fees from Spyryx Biosciences, personal fees from Vertex Pharmaceuticals, personal fees from Santhera, personal fees from Galapagos, personal fees from Sterna Biologicals, personal fees from Enterprise Therapeutics, personal fees from Celtaxys, outside the submitted work.

References

1. **Onland W, Debray TP, Laughon MM, Miedema M, Cools F, Askie LM, Asselin JM, Calvert SA, Courtney SE, Dani C, Durand DJ, Marlow N, Peacock JL, Pillow JJ, Soll RF, Thome UH, Truffert P, Schreiber MD, Van Reempts P, Vendettuoli V, Vento G, van Kaam AH, Moons KG, and Offringa M**. Clinical prediction models for bronchopulmonary dysplasia: a systematic review and external validation study. *BMC Pediatr* 13: 207, 2013.

2. **May C, Prendergast M, Salman S, Rafferty GF, and Greenough A**. Chest radiograph thoracic areas and lung volumes in infants developing bronchopulmonary dysplasia. *Pediatr Pulmonol* 44: 80-85, 2009.

3. **Washko GR**. Diagnostic imaging in COPD. *Semin Respir Crit Care Med* 31: 276-285, 2010.

4. **Ochiai M, Hikino S, Yabuuchi H, Nakayama H, Sato K, Ohga S, and Hara T**. A new scoring system for computed tomography of the chest for assessing the clinical status of bronchopulmonary dysplasia. *J Pediatr* 152: 90-95, 95 e91-93, 2008.

5. **Shin SM, Kim WS, Cheon JE, Kim HS, Lee W, Jung AY, Kim IO, and Choi JH**. Bronchopulmonary dysplasia: new high resolution computed tomography scoring system and correlation between the high resolution computed tomography score and clinical severity. *Korean J Radiol* 14: 350-360, 2013.

6. **Weatherley ND, Eaden JA, Stewart NJ, Bartholmai BJ, Swift AJ, Bianchi SM, and Wild JM**. Experimental and quantitative imaging techniques in interstitial lung disease. *Thorax* 74: 611-619, 2019.

7. **Jobe AH, and Bancalari E**. Bronchopulmonary dysplasia. *Am J Respir Crit Care Med* 163: 1723-1729, 2001.

8. **Forster K, Sass S, Ehrhardt H, Mous DS, Rottier RJ, Oak P, Schulze A, Flemmer AW, Gronbach J, Hubener C, Desai T, Eickelberg O, Theis FJ, and Hilgendorff A**. Early Identification of Bronchopulmonary Dysplasia Using Novel Biomarkers by Proteomic Screening. *Am J Respir Crit Care Med* 197: 1076-1080, 2018.

9. **Wielputz MO, Puderbach M, Kopp-Schneider A, Stahl M, Fritzsching E, Sommerburg O, Ley S, Sumkauskaite M, Biederer J, Kauczor HU, Eichinger M, and Mall MA**. Magnetic resonance imaging detects changes in structure and perfusion, and response to therapy in early cystic fibrosis lung disease. *Am J Respir Crit Care Med* 189: 956-965, 2014.

10. **De Boeck K, Derichs N, Fajac I, de Jonge HR, Bronsveld I, Sermet I, Vermeulen F, Sheppard DN, Cuppens H, Hug M, Melotti P, Middleton PG, Wilschanski M, Group EDNW, and EuroCare CFWPGoCFd**. New clinical diagnostic procedures for cystic fibrosis in Europe. *J Cyst Fibros* 10 Suppl 2: S53-66, 2011.

11. **Hirtz S, Gonska T, Seydewitz HH, Thomas J, Greiner P, Kuehr J, Brandis M, Eichler I, Rocha H, Lopes AI, Barreto C, Ramalho A, Amaral MD, Kunzelmann K, and Mall M**. CFTR Cl- channel function in native human colon correlates with the genotype and phenotype in cystic fibrosis. *Gastroenterology* 127: 1085-1095, 2004.

12. **Förster K, Ertl-Wagner B, Ehrhardt H, Busen H, Sass S, Pomschar A, Naehrlich L, Schulze A, Flemmer AW, Hübener C, Eickelberg O, Theis F, Dietrich O, and A. H**. Altered relaxation times in MRI indicate bronchopulmonary dysplasia. *Thorax* thoraxjnl-2018-212384.: 2019.

13. **Eichinger M, Optazaite DE, Kopp-Schneider A, Hintze C, Biederer J, Niemann A, Mall MA, Wielputz MO, Kauczor HU, and Puderbach M**. Morphologic and functional scoring of cystic fibrosis lung disease using MRI. *Eur J Radiol* 81: 1321-1329, 2012.

20

512 14.   **Kubota J, Ohki Y, Inoue T, Sakurai M, Shigeta M, Mochizuki H, Aoki J,**
513 **Morikawa A, and Endo K**. Ultrafast CT scoring system for assessing bronchopulmonary
514 dysplasia: reproducibility and clinical correlation. *Radiat Med* 16: 167-174, 1998.
515 15.   **Likert R**. *A technique for the measurement of attitudes*. New York,: 1932, p. 55 p.
516 16.   **Higano NS, Spielberg DR, Fleck RJ, Schapiro AH, Walkup LL, Hahn AD, Tkach**
517 **JA, Kingma PS, Merhar SL, Fain SB, and Woods JC**. Neonatal Pulmonary Magnetic
518 Resonance Imaging of Bronchopulmonary Dysplasia Predicts Short-Term Clinical
519 Outcomes. *Am J Respir Crit Care Med* 198: 1302-1311, 2018.
520 17.   **Baud O, Laughon M, and Lehert P**. Survival without Bronchopulmonary
521 Dysplasia of Extremely Preterm Infants: A Predictive Model at Birth. *Neonatology* 118:
522 385-393, 2021.
523 18.   **Breimann L, Friedmann JH, Olshen RA, and Stone CJ**. Classification and
524 Regression Trees. Monterey, CA: Wadsworth & Brooks/Cole Advanced Books &
525 Software; 1984.
526 19.   **Fahrmeir L**. *Regression : models, methods and applications*. New York: Springer,
527 2013.
528 20.   **Youden WJ**. Index for rating diagnostic tests. *Cancer* 3: 32-35, 1950.
529 21.   **Coalson JJ**. Pathology of bronchopulmonary dysplasia. *Semin Perinatol* 30: 179-
530 184, 2006.
531 22.   **Thebaud B, Goss KN, Laughon M, Whitsett JA, Abman SH, Steinhorn RH,**
532 **Aschner JL, Davis PG, McGrath-Morrow SA, Soll RF, and Jobe AH**. Bronchopulmonary
533 dysplasia. *Nat Rev Dis Primers* 5: 78, 2019.
534 23.   **Mizikova I, and Morty RE**. The Extracellular Matrix in Bronchopulmonary
535 Dysplasia: Target and Source. *Front Med (Lausanne)* 2: 91, 2015.
536 24.   **Grum CM, and Lynch JP, 3rd**. Chest radiographic findings in cystic fibrosis.
537 *Semin Respir Infect* 7: 193-209, 1992.
538 25.   **Fitzgerald DA, Van Asperen PP, Lam AH, De Silva M, and Henderson-Smart**
539 **DJ**. Chest radiograph abnormalities in very low birthweight survivors of chronic
540 neonatal lung disease. *J Paediatr Child Health* 32: 491-494, 1996.
541 26.   **Oda K, Ishimoto H, Yatera K, Naito K, Ogoshi T, Yamasaki K, Imanaga T,**
542 **Tsuda T, Nakao H, Kawanami T, and Mukae H**. High-resolution CT scoring system-
543 based grading scale predicts the clinical outcomes in patients with idiopathic pulmonary
544 fibrosis. *Respir Res* 15: 10, 2014.
545 27.   **Tulek B, Kivrak AS, Ozbek S, Kanat F, and Suerdem M**. Phenotyping of chronic
546 obstructive pulmonary disease using the modified Bhalla scoring system for high-
547 resolution computed tomography. *Can Respir J* 20: 91-96, 2013.
548 28.   **Sileo C, Corvol H, Boelle PY, Blondiaux E, Clement A, and Ducou Le Pointe H**.
549 HRCT and MRI of the lung in children with cystic fibrosis: comparison of different
550 scoring systems. *J Cyst Fibros* 13: 198-204, 2014.
551 29.   **Walkup LL, Tkach JA, Higano NS, Thomen RP, Fain SB, Merhar SL, Fleck RJ,**
552 **Amin RS, and Woods JC**. Quantitative Magnetic Resonance Imaging of
553 Bronchopulmonary Dysplasia in the Neonatal Intensive Care Unit Environment. *Am J*
554 *Respir Crit Care Med* 192: 1215-1222, 2015.
555 30.   **Semple T, Akhtar MR, and Owens CM**. Imaging Bronchopulmonary Dysplasia-A
556 Multimodality Update. *Front Med (Lausanne)* 4: 88, 2017.
557 31.   **Hahn AD, Higano NS, Walkup LL, Thomen RP, Cao X, Merhar SL, Tkach JA,**
558 **Woods JC, and Fain SB**. Pulmonary MRI of neonates in the intensive care unit using 3D
559 ultrashort echo time and a small footprint MRI system. *J Magn Reson Imaging* 45: 463-
560 471, 2017.

561 32.   **Havsteen I, Ohlhues A, Madsen KH, Nybing JD, Christensen H, and**
562 **Christensen A**. Are Movement Artifacts in Magnetic Resonance Imaging a Real
563 Problem?-A Narrative Review. *Front Neurol* 8: 232, 2017.
564 33.   **Oulego-Erroz I, Alonso-Quintela P, Terroba-Seara S, Jimenez-Gonzalez A,**
565 **and Rodriguez-Blanco S**. Early assessment of lung aeration using an ultrasound score
566 as a biomarker of developing bronchopulmonary dysplasia: a prospective observational
567 study. *J Perinatol* 41: 62-68, 2021.
568 34.   **Baraldi E, and Filippone M**. Chronic lung disease after premature birth. *N Engl J*
569 *Med* 357: 1946-1955, 2007.
570 35.   **Bourbon JR, Boucherat O, Boczkowski J, Crestani B, and Delacourt C**.
571 Bronchopulmonary dysplasia and emphysema: in search of common therapeutic targets.
572 *Trends Mol Med* 15: 169-179, 2009.
573 36.   **Doyle LW, Faber B, Callanan C, Freezer N, Ford GW, and Davis NM**.
574 Bronchopulmonary dysplasia in very low birth weight subjects and lung function in late
575 adolescence. *Pediatrics* 118: 108-113, 2006.
576 37.   **Davidson LM, and Berkelhamer SK**. Bronchopulmonary Dysplasia: Chronic
577 Lung Disease of Infancy and Long-Term Pulmonary Outcomes. *J Clin Med* 6: 2017.
578 38.   **Manja V, Lakshminrusimha S, and Cook DJ**. Oxygen saturation target range for
579 extremely preterm infants: a systematic review and meta-analysis. *JAMA Pediatr* 169:
580 332-340, 2015.
581 39.   **Gortner L, Misselwitz B, Milligan D, Zeitlin J, Kollee L, Borech K, Agostino R,**
582 **Van Reempts P, Chabernaud JL, Breart G, Papiernik E, Jarreau PH, Carrapato M,**
583 **Gadzinowski J, and Draper I**. Rates of bronchopulmonary dysplasia in very preterm
584 neonates in Europe: results from the MOSAIC cohort. *Neonatology* 99: 112-117, 2011.
585 40.   **Payne NR, LaCorte M, Sun S, Karna P, Lewis-Hunstiger M, Goldsmith JP, and**
586 **Breathsavers G**. Evaluation and development of potentially better practices to reduce
587 bronchopulmonary dysplasia in very low birth weight infants. *Pediatrics* 118 Suppl 2:
588 S65-72, 2006.
589 41.   **Siffel C, Kistler KD, Lewis JFM, and Sarda SP**. Global incidence of
590 bronchopulmonary dysplasia among extremely preterm infants: a systematic literature
591 review. *J Matern Fetal Neonatal Med* 1-11, 2019.
592 42.   **Couchard M, Polge J, and Bomsel F**. [Hyaline membrane disease: diagnosis,
593 radiologic surveillance, treatment and complications]. *Ann Radiol (Paris)* 17: 669-683,
594 1974.
595 43.   **Franz AR, Steinbach G, Kron M, and Pohlandt F**. Interleukin-8: a valuable tool
596 to restrict antibiotic therapy in newborn infants. *Acta Paediatr* 90: 1025-1032, 2001.
597 44.   **Sherman MP, Goetzman BW, Ahlfors CE, and Wennberg RP**. Tracheal
598 asiration and its clinical correlates in the diagnosis of congenital pneumonia. *Pediatrics*
599 65: 258-263, 1980.
600

601

602

603

604

605

606

607

22

Captions:

Table 1: Data are given as median and range or number and percent of total in group respective range. The percentage of BPD grades refers to the proportion of the respective BPD grade in relation to the total number of patients.

GA, gestational age; ANCS, antenatal corticosteroids; RDS, respiratory distress syndrome; ROP, retinopathy of prematurity; ICU, intensive care unit; BPD, bronchopulmonary dysplasia. Intrauterine growth restriction (IUGR) was defined as birth weight below the 10th percentile. Postnatally, diagnosis and severity of respiratory distress syndrome (RDS) were scored on anterior-posterior (a.-p.) chest radiographs according to Couchard et al (42). Chorioamnionitis was defined as inflammatory alterations of the chorionic plate (histologic examination) or signs of maternal and fetal signs of infection (43). Systemic infections were diagnosed according to Sherman et al. (44) based on one or more clinical and laboratory signs of infection. BPD was defined according to Jobe and Bancalari (7) and graded as mild (oxygen supplementation for at least 28 days postnatally=BPD grade 1), moderate (oxygen supplementation < 30% at 36 weeks postmenstrual age=BPD grade 2), and severe (oxygen supplementation > 30% and/or ventilator support at 36 weeks postmenstrual age=BPD grade 3).

Table 2: A) Representative lung MRIs of infants in coronal planes at the time of BPD diagnosis: (a) example of an emphysematous score of 4.5, (b) example of an interstitial enhancement score of 5, (c) example of an accentuated airway score of 3.5 (diaphragm blurring as a results of movement artefacts) and (d) example of a ventilation inhomogeneity score of 5 (thoracic wall double contours result from movement artefacts). B) Definition of the MRI score variables 'emphysema' (reduced signal intensity, rarefied lung vasculature, hyperexpansion, mosaic pattern of lung attenuation, bullae or blebs), 'interstitial enhancement' (distinctive representation of intestinal structures, thickening of bronchovascular bundle), 'airway accentuation' (increased signal intensity in the respiratory ducts, airway wall thickness in relation to airway), 'ventilation inhomogeneity' (caudo-cranial and anterior-to-posterior gradient of signal intensities). Scoring is achieved by the means of a 5-point- Likert scale with 1 reflecting physiologic result and 5 referring to maximum pathology. The variables

23

641   are assessed for each of the four lung quadrants separately.

642   BPD=Bronchopulmonary Dysplasia; MRI=Magnetic Resonance Imaging.

643

644   **Table 3:** Regression coefficients of the logistic models. Within the analysis the

645   threshold for the negative predictive value (NPV) and the positive predictive value

646   (PPV) were chosen by Youden index (20) when comparing no or mild with moderate

647   or severe cases. AIC=Akaike information criterion; BPD=bronchopulmonary

648   dysplasia; BPD grades: 0=no BPD, 1=mild BPD, 2=moderate BPD, 3=severe BPD;

649   logLik=logarithm of the likelihood.

650

651   **Figure 1: A)** Increased scores for 'airway accentuation', 'emphysema', 'interstitial

652   enhancement', and 'ventilation inhomogeneity' in infants with BPD when compared to

653   preterm infants without BPD. Points indicate individual cases. Median, 25 and 75%

654   quartiles, whiskers represent 1.5 times the interquartile range (IQR) (Pairwise

655   wilcoxon test with Bonferroni correction for multiple testing). **B)** Classification tree for

656   the binary outcome BPD (no and mild vs. moderate and severe BPD) with scoring

657   values as explanatory variables under consideration of GA and gender. Infants <26.0

658   weeks GA at birth with moderate or severe BPD were characterised by an increased

659   score for ‚emphysema' (≥1.88) in contrast to infants born >26.0 weeks GA that

660   predominantly revealed signs of ‚interstitial enhancement' when diagnosed with

661   moderate or severe BPD (≥3.13). In more mature infants (28th-29th weeks GA at

662   birth) with reduced presence of 'interstitial enhancement' (split value < 3.13),

663   increased 'ventilation inhomogeneity' (split value > 1.88) separated cases with

664   moderate or severe BPD from no or mild BPD (AUC 0.69 [0.58; 0.80]. AUC=Area

665   under the curve; BPD=bronchopulmonary dysplasia; BPD grades: 0=no BPD, 1=mild

666   BPD, 2=moderate BPD, 3=severe BPD; CART=Classification and Regression Tree;

667   GA=gestational age.

668   A prediction rule was deducted to detect disease grades using the score obtained for

669   the indicated variables. For CART model validation, a nested LOO cross-validation

670   with grid hyperparameter tuning was used to obtain the best performing model for the

671   binary value while displaying only relevant variables in the final tree.

672

673

674 **Figure 2: A)** Classification tree for the binary outcome BPD (no BPD vs. severe
675 BPD) with scoring values as explanatory variables under consideration of GA and
676 gender. BPD cases were separated by GA and 'interstitial enhancement' with a
677 validation AUC of 0.87 [0.70; 1]. Each node reports the ratio of infants with the
678 indicated outcome in relation to the total number of patients studied. **B)** Characteristic
679 curve patterns shaped by the mean of the scoring variables obtained in the different
680 disease groups (95% confidence intervals in grey): BPD (mild, moderate, severe) and
681 CF. **C)** Classification tree for the binary outcome disease type, i.e., BPD and CF with
682 scoring values as explanatory variables. Disease types were separated by the score
683 variables 'emphysema' and 'ventilation inhomogeneity' (AUC 0.91 [0.82; 0.99], split
684 values <1.13 and ≥1.75). **A+C:** Each node reports the ratio of infants with the
685 indicated outcome in relation to the total number of infants studied. AUC=Area under
686 the curve; BPD=bronchopulmonary dysplasia; BPD grades: 0=no BPD, 1=mild BPD,
687 2=moderate BPD, 3=severe BPD; CART=Classification and Regression Tree;
688 CF=Cystic Fibrosis; GA=gestational age.
689 A prediction rule was deducted to detect disease grades using the score obtained for
690 the indicated variables. For CART model validation, a nested LOO cross-validation
691 with grid hyperparameter tuning was used to obtain the best performing model for the
692 binary value while displaying only relevant variables in the final tree.
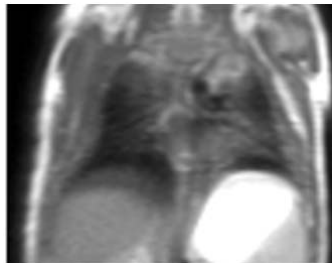693

Table 1. Patient characteristics

	no BPD	BPD 1	BPD 2+3	BPD 3
n	32 (38.1%)	25 (29.8%)	27 (32.1%)	18 (21.4%)
GA (weeks)	29.3 (27.0-31.3)	26.2 (24.1-29.4)	25.3 (23.2-28.5)	25.6 (23.2-28.4)
Birth weight (g)	1190 (700-1770)	780 (580-1510)	680 (300-1000)	705 (300-925)
IUGR	2 (6,3%)	1 (4%)	6 (22.2%)	5 (27.8%)
Gender (female/male)	16/16	8/17	14/13	9/9
ANCS	28 (87.5%)	20 (80%)	22 (81.5%)	14 (77.8%)
Chorioamnionitis	11 (34.4%)	17 (68%)	15 (55.6%)	9 (50%)
Early onset infection	5 (15.6%)	10 (40%)	10 (37%)	7 (38.9%)
RDS ≥ grade3	3 (9.4%)	7 (28%)	12 (44.4%)	6 (33.3%)
Days of mechanical ventilation	16 (0-52)	49 (17-63)	72 (7-129)	71 (7-129)
- Endotracheal ventilation	0 (0-11)	3 (0-22)	24 (0-44)	27 (0-44)
- Pharyngeal ventilation	15 (0-51)	41 (14-59)	45 (7-102)	45 (7-102)
Postnatal Steroids	6 (18.8%)	9 (36%)	17 (63%)	12 (66.7%)
ROP ≥ 3	1 (3.1%)	2 (8%)	6 (22.2%)	5 (27.8%)
ICU days	56 (13-142)	80 (26-120)	101 (22-150)	100 (22-150)

Data are given as median and range or number and percent of total in group respective range. The percentage of BPD grades refers to the proportion of the respective BPD grade in relation to the total number of patients.

GA, gestational age; ANCS, antenatal corticosteroids; RDS, respiratory distress syndrome; ROP, retinopathy of prematurity; ICU, intensive care unit; BPD, bronchopulmonary dysplasia. Intrauterine growth restriction (IUGR) was defined as birth weight below the 10th percentile. Postnatally, diagnosis and severity of respiratory distress syndrome (RDS) were scored on anterior-posterior (a.-p.) chest radiographs according to Couchard et al (42). Chorioamnionitis was defined as inflammatory alterations of the chorionic plate (histologic examination) or signs of maternal and fetal signs of infection (43). Systemic infections were diagnosed according to Sherman et al. (44) based on one or more clinical and laboratory signs of infection. BPD was defined according to Jobe and Bancalari (7) and graded as mild (oxygen supplementation for at least 28 days postnatally=BPD grade 1), moderate (oxygen supplementation < 30% at 36 weeks postmenstrual age=BPD grade 2), and severe (oxygen supplementation > 30% and/or ventilator support at 36 weeks postmenstrual age=BPD grade 3).

Table 2. MRI Scoring system for the semi-quantitative assessment of structural disease characteristics in preterm infants with BPD

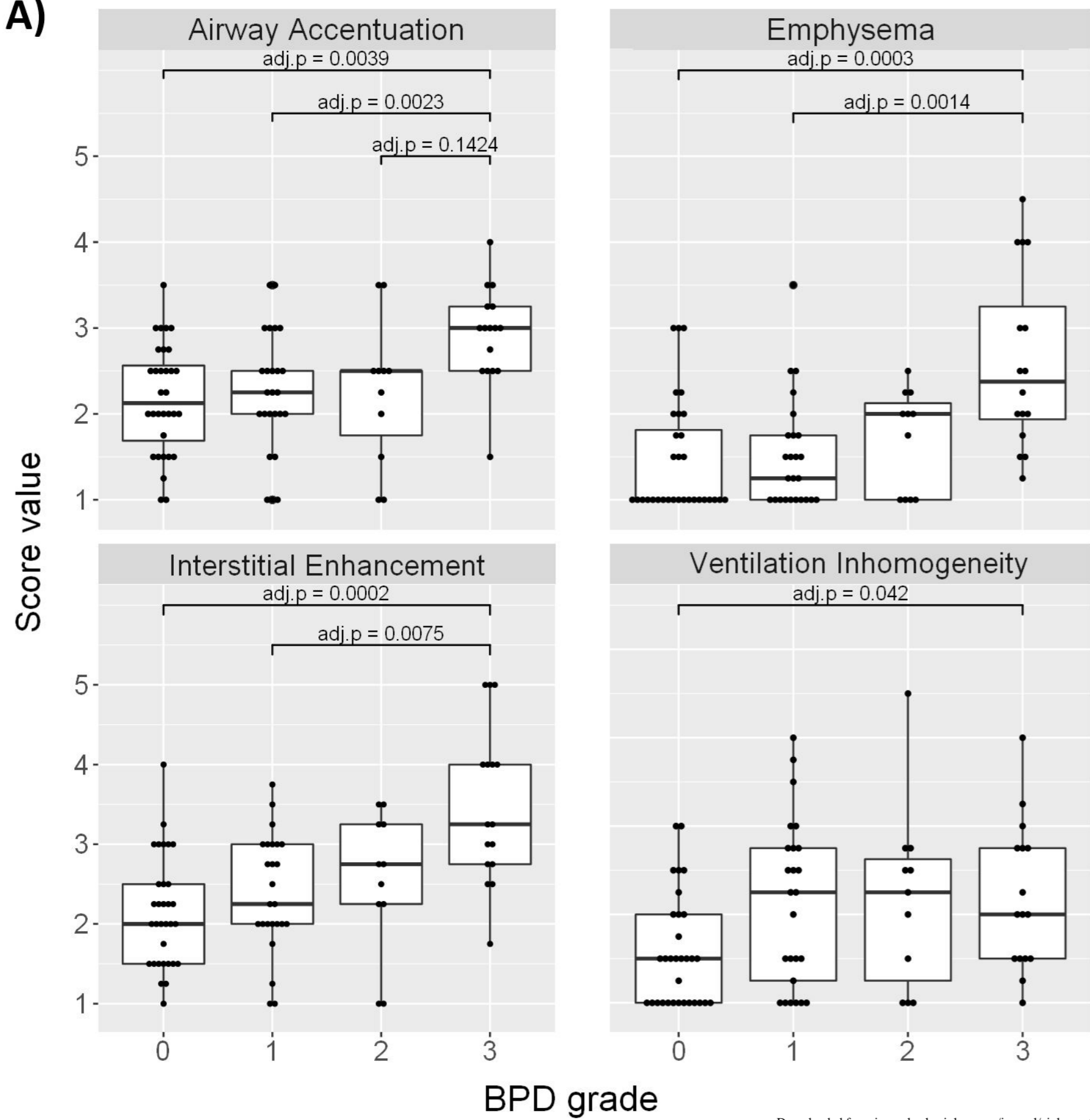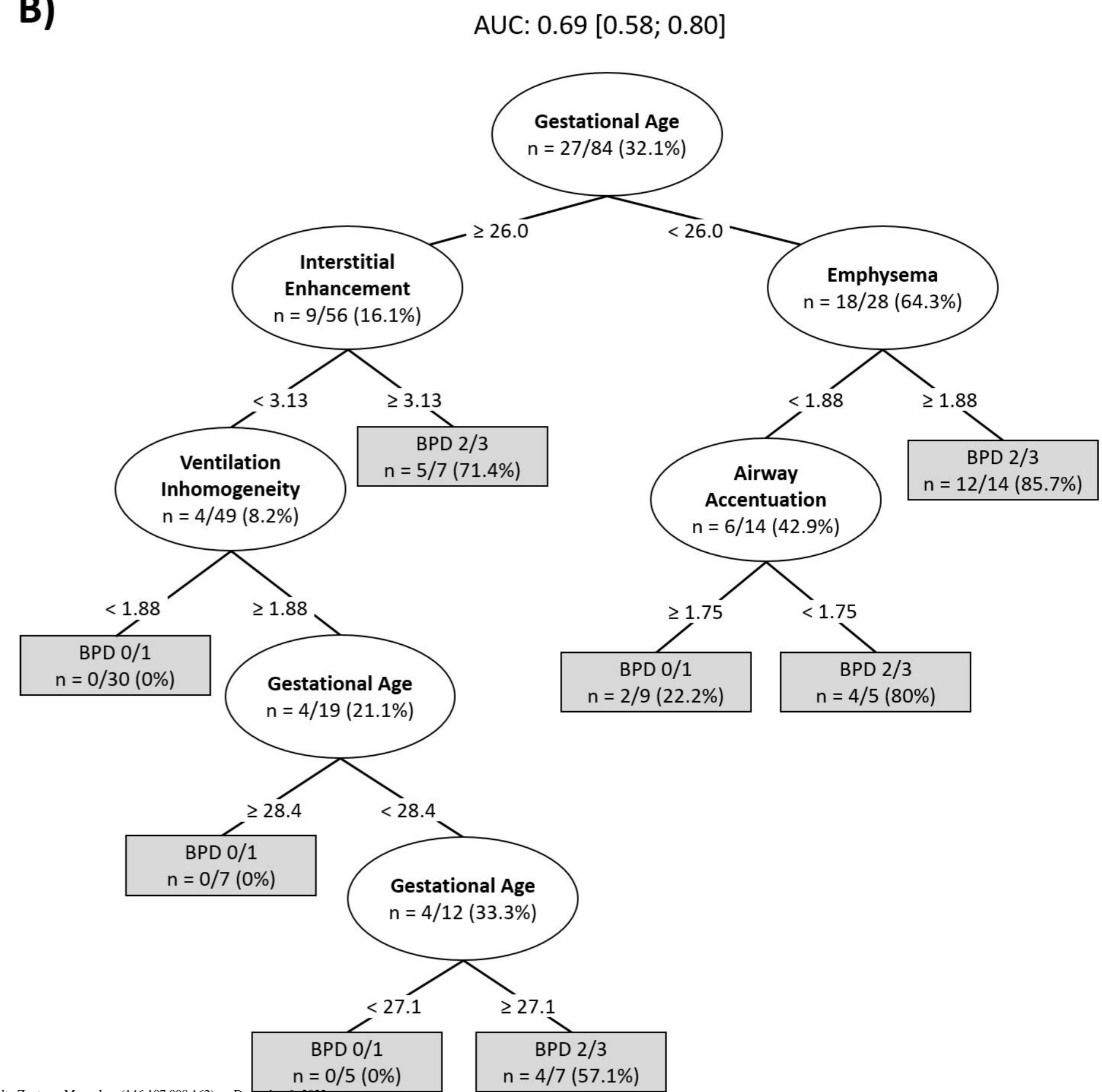| A) lung MRIs	a) emphysema (Score 4.5)	b) interstitial enhancement (Score 5)	c) airway accentuation (Score 3.5)	d) ventilation inhomogeneity (Score 5)
B) score				
1	none	none	none	none
2	central	central, patchy not homogeneous	2:1 in 1 quadrant	mild
3	approx. 50% of total lung area	approx. 50% of total lung area	2:1 in 2 quadrants	moderate
4	approx. 75% of total lung area	approx. 75% of total lung area	2:1 in 3 quadrants	severe
5	4 quadrants Intercostal bulging	central and peripheral, homogeneous	2:1 in 4 quadrants	global severe

Table 2: A) Representative lung MRIs of infants in coronal planes at the time of BPD diagnosis: (a) example of an emphysematous score of 4.5, (b) example of an interstitial enhancement score of 5, (c) example of an accentuated airway score of 3.5 (diaphragm blurring as a results of movement artefacts) and (d) example of a ventilation inhomogeneity score of 5 (thoracic wall double contours result from movement artefacts). **B)** Definition of the MRI score variables 'emphysema' (reduced signal intensity, rarefied lung vasculature, hyperexpansion, mosaic pattern of lung attenuation, bullae or blebs), 'interstitial enhancement' (distinctive representation of intestinal structures, thickening of bronchovascular bundle), 'airway accentuation' (increased signal intensity in the respiratory ducts, airway wall thickness in relation to airway), 'ventilation inhomogeneity' (caudo-cranial and anterior-to-posterior gradient of signal intensities). Scoring is achieved by the means of a 5-point- Likert scale with 1 reflecting physiologic result and 5 referring to maximum pathology. The variables are assessed for each of the four lung quadrants separately. BPD=Bronchopulmonary Dysplasia; MRI=Magnetic Resonance Imaging.
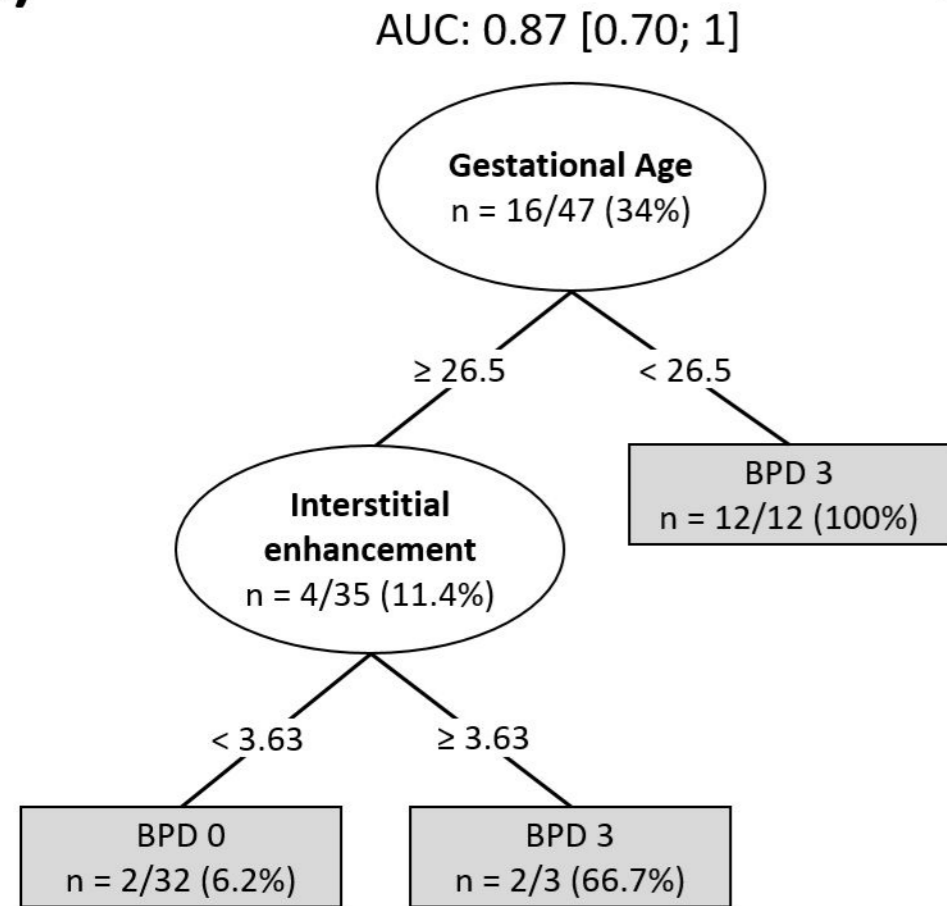
Table 3. Results of logistic regression models

	BPD 01 vs. 23	Model BPD 0 vs. 3
(Intercept)	16.616 **	39.527 *
	(5.228)	(17.339)
Emphysema	1.108	0.408
	(0.629)	(1.148)
Interstitial Enhancement	0.287	0.338
	(0.524)	(0.927)
Airway Accentuation	0.425	1.387
	(0.575)	(1.715)
Ventilation inhomogeneity	-0.483	1.138
	(0.481)	(1.212)
Gestational Age	-0.750 ***	-1.725 *
	(0.200)	(0.673)
Gender (male)	-0.165	-0.474
	(0.698)	(1.818)
N	84	48
logLik	-31.818	-7.638
AIC	77.636	29.276

*** p < 0.001; ** p < 0.01; * p < 0.05.

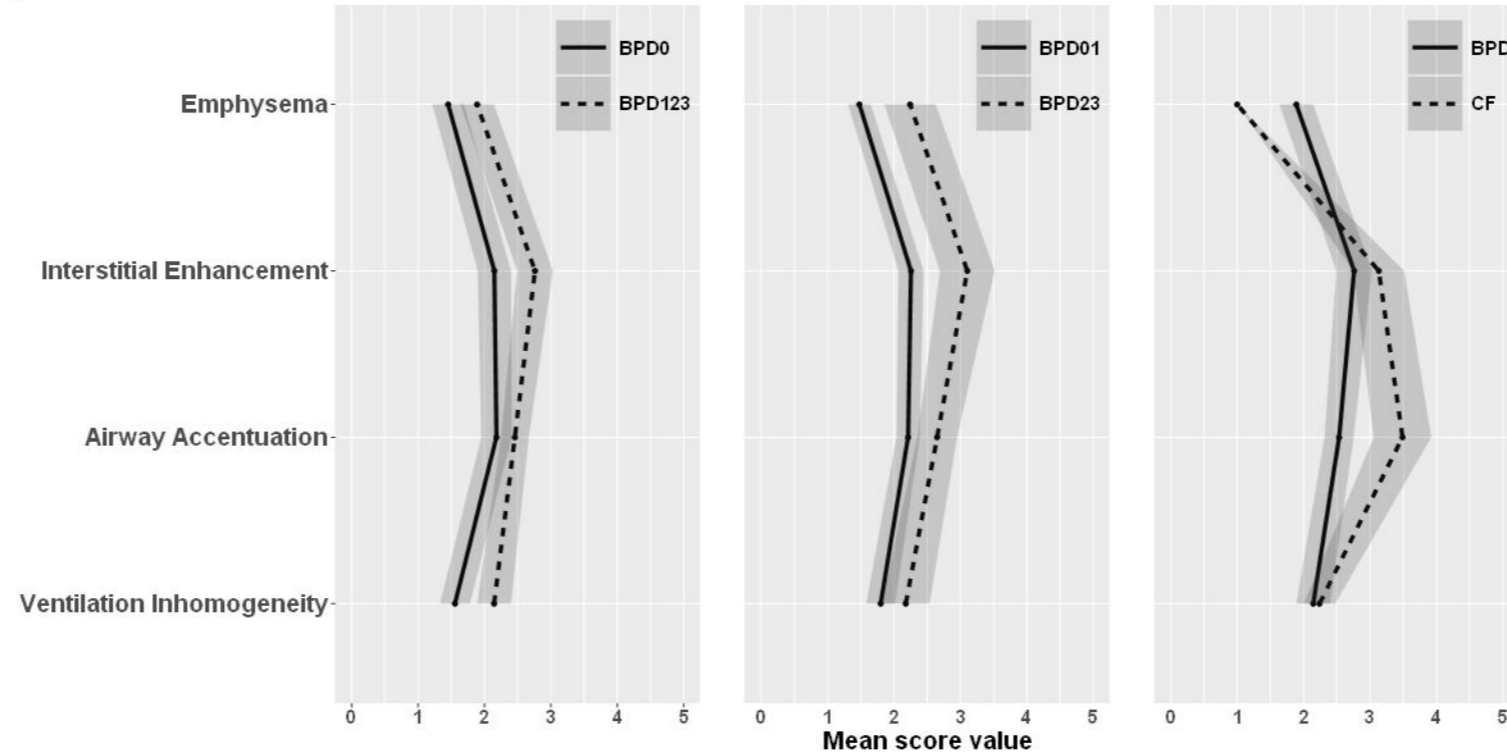Table 3: Regression coefficients of the logistic models. Within the analysis the threshold for the negative predictive value (NPV) and the positive predictive value (PPV) were chosen by Youden index (20) when comparing no or mild with moderate or severe cases. AIC=Akaike information criterion; BPD=bronchopulmonary dysplasia; BPD grades: 0=no BPD, 1=mild BPD, 2=moderate BPD, 3=severe BPD; logLik=logarithm of the likelihood.

A)

Airway Accentuation
adj.p = 0.0039
adj.p = 0.0023
adj.p = 0.1424

Emphysema
adj.p = 0.0003
adj.p = 0.0014

Interstitial Enhancement
adj.p = 0.0002
adj.p = 0.0075

Ventilation Inhomogeneity
adj.p = 0.042

Score value

BPD grade

B)

AUC: 0.69 [0.58; 0.80]

Gestational Age
n = 27/84 (32.1%)

≥ 26.0 / < 26.0

Interstitial Enhancement
n = 9/56 (16.1%)

Emphysema
n = 18/28 (64.3%)

< 3.13 / ≥ 3.13

Ventilation Inhomogeneity
n = 4/49 (8.2%)

BPD 2/3
n = 5/7 (71.4%)

< 1.88 / ≥ 1.88

< 1.88 / ≥ 1.88

Airway Accentuation
n = 6/14 (42.9%)

BPD 2/3
n = 12/14 (85.7%)

BPD 0/1
n = 0/30 (0%)

Gestational Age
n = 4/19 (21.1%)

≥ 1.75 / < 1.75

BPD 0/1
n = 2/9 (22.2%)

BPD 2/3
n = 4/5 (80%)

≥ 28.4 / < 28.4

BPD 0/1
n = 0/7 (0%)

Gestational Age
n = 4/12 (33.3%)

< 27.1 / ≥ 27.1

BPD 0/1
n = 0/5 (0%)

BPD 2/3
n = 4/7 (57.1%)

A) AUC: 0.87 [0.70; 1]

Gestational Age
n = 16/47 (34%)

≥ 26.5 / < 26.5

Interstitial enhancement
n = 4/35 (11.4%)

BPD 3
n = 12/12 (100%)

< 3.63 / ≥ 3.63

BPD 0
n = 2/32 (6.2%)

BPD 3
n = 2/3 (66.7%)

C) AUC: 0.91 [0.82; 0.99]

Emphysema
n = 21/73 (28.8%)

≥ 1.13 / < 1.13

BPD
n = 0/38 (0%)

Ventilation Inhomogeneity
n = 21/35 (60%)

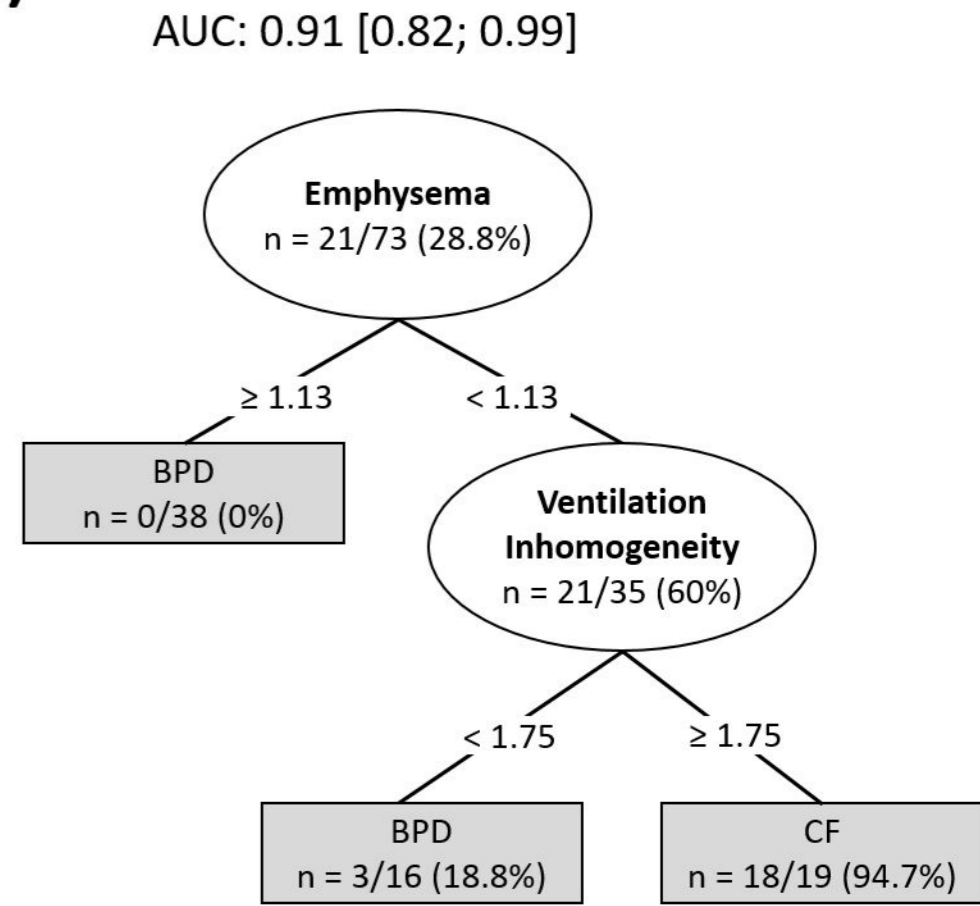< 1.75 / ≥ 1.75

BPD
n = 3/16 (18.8%)
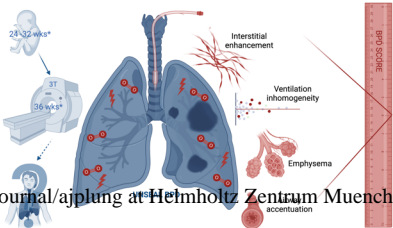
CF
n = 18/19 (94.7%)

UNiforme **S**coring of the dis**EA**sed Lung in BPD

Increased scores for 'emphysema' and 'airway accentuation' (extremely premature), 'interstitial enhancement' and 'ventilation inhomogeneity' (very premature) characterize BPD.

24-32 wks*

3T

36 wks*

Interstitial enhancement

Ventilation inhomogeneity

Emphysema

accentuation

BPD SCORE

journal/ajplung at Helmholtz Zentrum Muenche

*postmenstrual age (PMA)